13th International Conference on
Structural Health Monitoring of Intelligent Infrastructure
DOI: 10.3217/978-3-99161-057-1-020

Water distribution pipeline anomaly detection using distributed acoustic sensing (DAS)

Maksymilian Jasiak [1], Shih-Hung Chiu[1], Jaewon Saw[1], Peter Hubbard[2], David Katzev[3], Kenichi Soga[1]
[1]Department of Civil and Environmental Engineering, University of California, Berkeley, USA
[2]FiberSense, USA
[3]East Bay Municipal Utility District, USA
email: jasiak@berkeley.edu, shchiu@berkeley.edu, jaewon.saw@berkeley.edu,
peter.hubbard@fibersense.com, david.katzev@ebmud.com, soga@berkeley.edu

ABSTRACT: Leak detection for water pipelines, and anomaly detection more broadly, is vital to ensuring reliable access to drinking water. Monitoring transmission and distribution pipelines supports proactive fault detection to reduce water loss amid deteriorating infrastructure and depleting water resources. Distributed acoustic sensing (DAS) in the form of phase-sensitive optical time-domain reflectometry (φ-OTDR) can quantify vibrations and sound along fiber optic cables over long distances with high spatial resolution and frequency. In this study, DAS was deployed on a new fiber optic cable-instrumented pipeline to investigate DAS sensitivity to pipe water leakage noise. A reproducible workflow for system deployment and signal processing aimed at pipe water leak detection in field conditions is presented. The influence of fiber optic cable type (tight-buffered vs. loose tube) and installation condition (pipe-mounted vs. trench-lain) on DAS sensitivity was assessed during pipe water filling and simulated leakage. Findings demonstrate relatively high sensitivity to water leak noise detection when DAS is deployed on fiber optic cables near the pipeline. This informs best practices for data-driven pipeline monitoring by presenting a reproducible procedure to operationalize water pipeline leak detection using DAS.

KEY WORDS: Water pipeline leak detection; Distributed fiber optic sensing (DFOS); Distributed acoustic sensing (DAS).

1 INTRODUCTION

Water leak detection on transmission and distribution pipeline networks is critical to reduce water loss. Growing challenges, such as deteriorating infrastructure and depleting water resources, highlight the need for resilient water infrastructure to ensure reliable access to drinking water. Proactive monitoring plays an important role in helping track down unaccounted non-revenue water losses across geographically distributed pipeline systems. Monitoring also helps water supply agencies effectively predict life expectancy and plan maintenance and rehabilitation of lifeline pipelines. Furthermore, water infrastructure monitoring in low-resource environments is vital for resilient asset management in vulnerable communities.

Conventional methods for pipeline water leak detection are often limited in their balance of scale or spatial resolution. Satellite sensing with synthetic aperture radar (SAR) as well as unmanned aerial vehicle (UAV) sensing with multi-spectral or thermal imaging can detect elevated levels of underground soil moisture caused by leaking water. These offer regional-scale monitoring, but at relatively low spatial resolution. Various pipe-mounted or in-pipe point sensors can detect leakage-related water pressure drops or acoustic emissions, but their scale and spatial resolution is dependent on sensor density (which scales poorly due to high installation and maintenance costs). Ground penetrating radar (GPR) to detect subsurface moisture and listening sticks to listen for water leakage noise can offer pipe segment scale and spatial resolution, but their large-scale deployment is constrained by slow manual labor. In short, conventional methods balance between scale and spatial resolution due to technical constraints. As a result, they typically need to be deployed in parallel to attempt comprehensive monitoring of entire pipeline networks.

However, regional-scale sensing with meter-level spatial resolution is in fact achievable with Distributed Fiber Optic Sensing (DFOS). This family of technologies is at the forefront of large-scale infrastructure performance monitoring of strain, temperature, vibrations, and sound along fiber optic cables over long distances at a high spatial resolution with high measurement frequencies [1]. Distributed acoustic sensing (DAS) in the form of phase-sensitive optical time-domain reflectometry (φ-OTDR) has proven uniquely suitable for vibration and sound monitoring of linear civil infrastructure such as offshore wind turbines [2][3], roadways [4], boreholes [5], and pipelines [6][7]. Furthermore, DAS has proven an effective tool even in noisy acoustic environments [8].

Previous work has investigated ground movement-induced pipeline deformation, a common cause of pipe water leakage, in both laboratory and field conditions using Distributed Strain and Temperature Sensing (DSTS) [9][10][11]. This study builds on this work to develop robust methods to directly investigate pipe water leakage by characterizing the distributed acoustic signal of typical and atypical pipeline activities. DAS was deployed on a new 120 m (394 ft) segment of 15.3 cm (6-inch) Earthquake Resistant Ductile Iron Pipe (ERDIP) in a residential neighborhood within the Hayward Fault Zone in Berkeley, California. This new pipeline replaced the old existing pipe which had previously experienced multiple main breaks and major leakage events.

Operationalizing DAS involves implementing an interpretable and reproducible workflow for system deployment and signal processing. Data gathering should be grounded in domain knowledge encompassing real world conditions and decisions and adaptable to past, present, and future data. Data processing should support: 1) predictable outputs withstanding scrutiny from reality checks; 2) computationally efficient use of data storage and processing resources; 3) stability under perturbations in input data and data

DOI: 10.3217/978-3-99161-057-1-020

gathering and processing judgement calls [12]. In this context, this study presents a reproducible workflow for DAS system deployment and signal processing aimed at pipe water leak detection in field conditions.

2 DAS METHOD

Distributed Fiber Optic Sensing (DFOS) quantifies backscattered light in optical fibers to quantify strain, temperature, or vibrations and sound. DFOS involves a sensing device (optical interrogator) connected to one end of a long linear sensor (fiber optic cable). The interrogator sends pulses of light through the optical fiber core of the cable. As these light pulses travel though the core, they interact with imperfections in the silica glass material and are backscattered. Light is backscattered in three typical mechanisms: Raman, Brillouin, and Rayleigh scattering. These mechanisms are sensitive to changes in temperature, strain, or vibrations/sound along the fiber. Rayleigh backscattered light is detected by the interrogator and processed with optical interferometry for distributed acoustic sensing (DAS) [1]. Specifically, phase-sensitive optical time-domain reflectometry (φ-OTDR) uses the phase change $\Delta\phi$ of coherent Rayleigh backscattering to quantify vibrations and sound as dynamic strain ε given a known operational wavelength λ, fiber refractive index n, gauge length G, and photoelastic scaling factor ξ [8].

$$\varepsilon = \frac{\lambda}{4\pi n G \xi}\Delta\phi \quad (1)$$

2.1 System selection

A DAS system includes a sensing device (optical interrogator) and sensor (fiber optic cable). Optical interrogator hardware and data acquisition parameter selection must ensure adequate sensing range, sampling frequency, spatial resolution, and sampling interval to capture the signal of interest. The sensing range must be sufficiently long to capture measurements along the entire sensing fiber. Sampling frequency should ensure sufficient temporal resolution to capture signals of interest at frequencies below the Nyquist frequency. For context, the Nyquist frequency is the highest frequency that can be accurately measured in a discrete signal and is typically defined as half the sampling frequency 0. In short, sampling frequency should be greater than double the expected frequency of the signal of interest. Spatial resolution (gauge length) [13] and sampling interval (gauge pitch or channel spacing) [14] depend on optoelectronic hardware component capabilities. In short, spatial resolution and sampling interval should be sufficiently low to capture localized signals along the fiber. Generally, data acquisition parameters are limited by hardware limitations and data processing constraints.

In this study, data acquisition parameters were set to a sampling frequency up to 100 kHz, a minimum spatial resolution of 2 m, and a minimum sampling interval of 1 m for 690 m total sensing fiber length using an OptaSense ODH4 DAS interrogator unit. Note, the 100 kHz raw ping rate was decimated down to 25 kHz during data acquisition and down to 5 kHz during data processing for reasons explained later.

Fiber optic cable selection must ensure proper protection of the optical fiber core and adequate coupling between the core and the external environment. Protecting the optical fiber core from moisture, chemicals and physical damage in the external environment is necessary to ensure fiber survival. This protection is achieved through various layers separating the central core from the outer cable jacket. Two typical protection designs are tight-buffered (Figure 1) and loose-tube (Figure 2). Tight-buffered cables tightly envelop the optical fiber with a plastic buffer to protect from moisture, steel reinforcement wires to protect from physical damage, and a plastic outer jacket to serve as a fluid barrier. Loose-tube cables loosely suspend the optical fiber with gel-filled tube to protect from excessive tension or bending, surrounded by aramid yard and a plastic outer jacket to protect from fluid moisture.

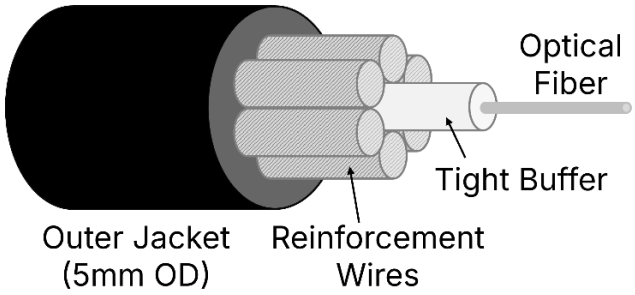

Figure 1. Tight-buffered fiber optic cable

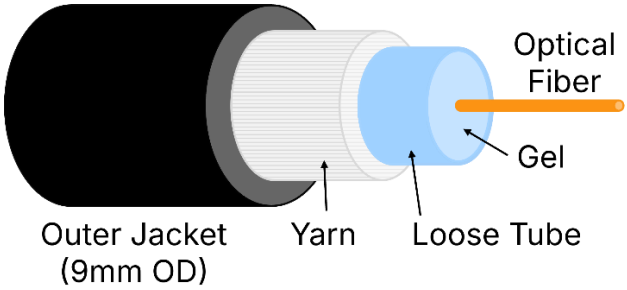

Figure 2. Loose-tube fiber optic cable

In terms of DFOS performance, the tight layer boundaries of tight-buffered cables provide a high degree of strain transfer from the outside environment to the fiber optical core. This enables high acoustic signal transmission from outside the cable to the fiber core. On the other hand, the gel-suspension layer boundary in loose-tube cables results in a significantly lower degree of strain transfer from the outside environment to the fiber optical core. This results in lower acoustic signal sensitivity from outside the cable to the fiber core.

In terms of durability and long-term environmental longevity, tight-buffered cables are more rugged and flexible during handling and installation but less resistant to extreme environmental conditions. On the other hand, loose-tube cables are more fragile during installation, but more resistant to hard environments with significant moisture and temperature changes. As a result, tight-buffered cables are typically used for DFOS applications or short-distance telecommunications, while loose-tube cables are used for long-distance telecommunications. Accordingly, tight-buffered cables are often more expensive due to lower niche demand, while loose-tube cables are more affordable given the high demand during mass deployment in global telecommunications networks.

In this study, tight-buffered cables and loose-tube fiber optic cables were both used to compare their DAS sensitivity to

DOI: 10.3217/978-3-99161-057-1-020

pipeline water leakage noise. Tight-buffered cables were sourced from NZ Sensing (NZS-DSS-C02). Loose-tube cables were sourced from Belden (FSSC002N0).

2.2 System deployment

DAS system sensitivity is influenced by the ability of the signal of interest to reach the fiber optic cable. The closer the cable sensor is to the signal source, the better the dynamic strain transfer-related acoustic signal transmission between the cable outer jacket and the fiber core, the better the DAS sensitivity.

If it is possible to install fiber optic cables designated for DAS directly on the monitored structure, they should be positioned as close as possible to the expected signal source location. Structure-mounted (or even structure-embedded) fiber optic cables intuitively offer the best DAS sensitivity. Installing both tight-buffered and loose-tube fiber optic cables supports DSTS (tight-buffered cables with high strain transfer for strain sensing vs. loose-tube cables with low strain transfer for temperature sensing). In the case of DAS, installing both enables a robust comparison between the two. However, deploying structure-mounted fiber optic cables has financial and logistical challenges due to the material and labor cost associated with custom installations.

Instead, existing buried fiber optic cables can be used. Conveniently, these existing cables are widespread under city streets in urban areas with fiber optic internet and telecommunications networks. This provides a cost-effective opportunity to deploy DAS on "dark" (currently unused) fibers in these existing cables without having to install new cables. However, deploying dark fiber DAS on existing telecommunications cables has two significant challenges: 1) existing cables may not be close to the monitored structure and 2) existing cables typically have a loose-tube (either gel-filled or air-filled) internal structure. This results in typically lower dark fiber DAS sensitivity using these types of existing cables.

In short, structure-mounted fiber optic cables offer superior DAS sensitivity but require resources to deploy, while existing buried fiber optic cables offer a convenient low-cost sensor but have lower DAS sensitivity. Using dark (unused) telecom fibers offer unique opportunities for widespread urban DAS activity monitoring. However, quantifying dark fiber DAS sensitivity to pipe water leakage remains a technical challenge.

In this study, both characteristic cable configurations were simulated to investigate their influence on DAS sensitivity to pipeline water leakage noise. Four sensing cable type and location configurations were deployed: 1) pipe-mounted tight-buffered; 2) pipe-mounted loose-tube; 3) trench-lain loose-tube; 4) trench-lain tight-buffered (Figure 3). Pipe-mounted cables were epoxied along the top of the pipe directly to the external pipe wall (Figure 4). A generic field-grade epoxy (toughened methacrylate adhesive system) was used to securely attach the fiber optic cables to the outer surface of the top of the pipe. Cables were aligned and epoxied straight along each approximately 6 m (20 ft) pipe segment. A small loop of slack cable was left at each joint between pipe segments to accommodate the discontinuity in the pipeline surface. Overall, the pipe-mounted cable installation process had a productivity of about 30 minutes per pipe segment. This time was primarily spent on placing and smoothing out the epoxy along the cables.

Trench-lain cables were aligned parallel to the pipeline and laid out on the bottom of the excavated pipe trench (Figure 5). This process was relatively fast and did not require any specialized tools. Reasonable effort was taken to ensure the cables were aligned straight along the pipeline with an approximately 5 cm offset from the side of the pipe.

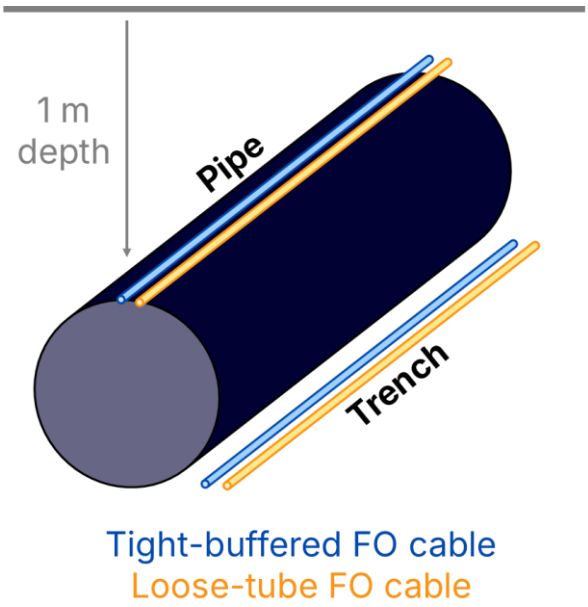

Figure 3. Fiber optic-instrumented pipeline

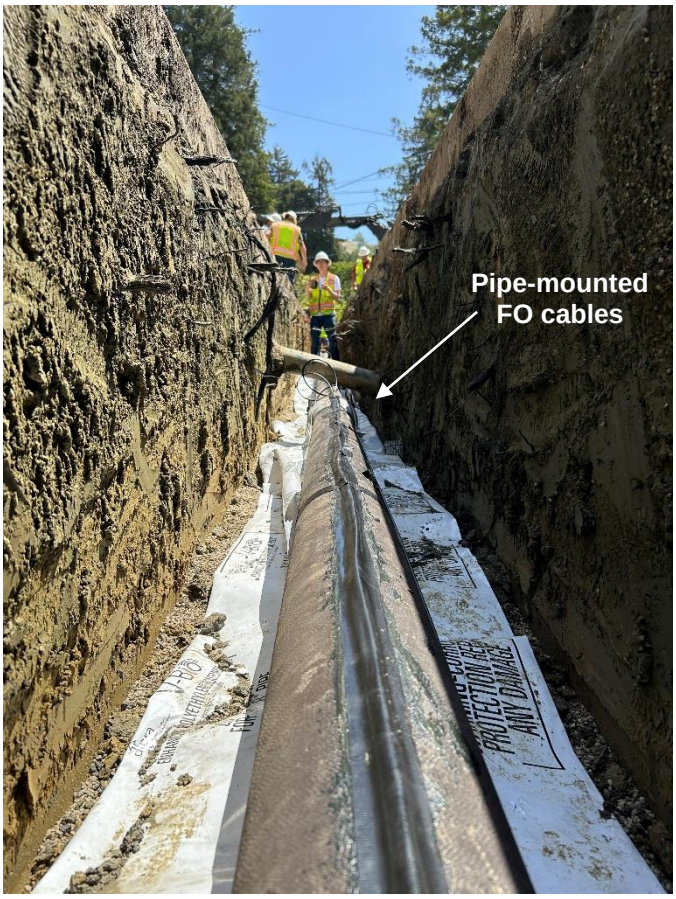

Figure 4. Pipe-mounted fiber optic cable installation

Regarding fiber protection, no additional protection measures were taken. This was to simulate a simple direct-

DOI: 10.3217/978-3-99161-057-1-020

burial fiber cable installation process. After fiber optic cables were epoxied to the pipeline and lain in the trench, the entire trench was backfilled with coarse sand. The backfill material (Class I backfill) is a typical crushed stone manufactured aggregate used in pipeline construction in the region. The trench backfill material was poured into the trench and was not compacted. A final thin layer of pavement subbase layer of course aggregate was placed on top of the trench backfill. This pavement subbase was compacted at the ground surface.

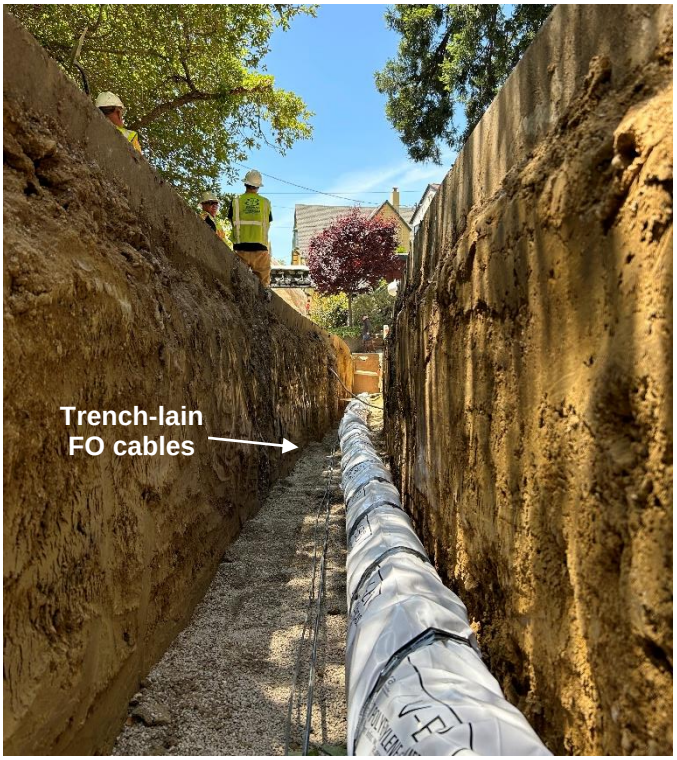

Figure 5. Trench-lain fiber optic cable installation

These four combinations were compared to investigate the influence of fiber-environment coupling conditions. Pipe-mounted cables were expected to exhibit higher DAS sensitivity to signals originating from the pipeline than trench-lain cables. Tight-buffered cables were expected to exhibit lower noise levels with a higher signal-to-noise (SNR) ratio than loose-tube cables with higher noise and lower SNR.

DAS measurements were performed during pipeline commissioning in which this 120-meter pipeline section was connected to the wider water distribution pipeline network. After the two ends of this pipeline was physically connected to the network with valves, the commissioning process involved 1) filling the empty pipe with water and 2) high flow flushing water through the pipe to flush out random debris.

During both tasks, a valve was opened at the downhill end of the pipe to allow water from the pressurized network to flow into the pipe, and a second valve at the uphill end of the pipe was open to air pressure. This water then flowed up into the pipe and filled the pipe with a velocity of approximately 0.7 m/s (2.3 ft/s). This filling process took approximately 180 seconds to fill 120 m of pipe. This meant that once the water level inside the pipeline reached the uphill valve, water would flow out to the ground surface. In the case of the second task, the high flow flushing process resulted in water violently erupting into the air (Figure 6). These conditions uniquely resembled a violent pipeline break and high flow pipe water leakage. This presented an opportunity to quantify DAS signal characteristics during simulated pipe water leakage.

Figure 6. Simulated leakage at uphill end pipe valve

2.3 Signal processing

Analysis of φ-OTDR DAS data started with downsampling the raw measured phase shift data to reduce dataset size while preserving key signal characteristics. The 100 kHz interrogator ping rate was decimated down to 25 kHz during data acquisition and down to 5 kHz during data processing to reduce computational costs and facilitate data handling. Data acquisition decimation was performed by a proprietary OptaSense algorithm inside the ODH4 operating software. Data processing decimation was performed by filtering (order 8 Chebyshev type I zero-phase anti-aliasing digital filter) and downsampling the signal. This effective sampling rate of 5 kHz with a Nyquist frequency of 2.5 kHz was sufficiently high to capture the relatively acoustic signal of pipeline water flow.

Next, phase change $\Delta\phi$ was related to dynamic strain ε as presented earlier (Equation 1). Next, frequency band extraction (FBE) was used to inspect the acoustic signal energy content at a specific frequency band appropriate for pipe water leakage noise. Given the dynamic strain spatial timeseries $x_{ch}(t)$ across time t for each channel location ch, each timeseries is divided into time frames and windowed with a periodic Hann window applied to each frame $w(t)$, and detrended by subtracting the mean value within the time frame μ_{ch}.

$$\tilde{x}_{ch}(t) = (x_{ch}(t) - \mu_{ch}) \cdot w(t) \quad (2)$$

Detrending helps remove low-frequency signal drift, while windowing helps reduce spectral leakage in the signal [12][15] . A Fast Fourier Transform (FFT) is then then applied to the detrended and windowed signal.

DOI: 10.3217/978-3-99161-057-1-020

$$X_{ch}(f) = FFT(\tilde{x}_{ch}(t)) \quad (3)$$

Next, the power spectrum for each channel is estimated on the FFT and scaled based on the FFT size $N_{FFT} = 256$, sampling frequency f_s, and energy correction factor $C_w = \sqrt{8/3}$ for Hann window coherency gain.

$$P_{ch}(f) = \frac{2}{N_{FFT} \cdot f_s} \cdot |X_{ch}(f)|^2 \cdot C_w \quad (4)$$

Afterwards, the frequency band extracted (FBE) power for each channel is extracted by averaging the power across the number of frequency bins N_f within the target frequency band from f_{min} to f_{max}.

$$FBE_{ch} = \frac{1}{N_f} \sum_{f_{min}}^{f_{max}} P_{ch}(f) \quad (5)$$

Finally, the mean FBE power in the frequency band is expressed on a logarithmic scale as decibels (dB).

$$FBE_{ch}^{dB} = 10 \log_{10} FBE_{ch} \quad (6)$$

Given the initial input strain spatial time series in units of microstrain $\mu\varepsilon$, the units of FBE power are $dB(\mu\varepsilon^2/Hz)$. The FBE power spatiotemporal trend was visualized along the entire fiber length using a waterfall plot format of space (y axis) vs. time (x axis) vs. FBE power (pixel color). This full fiber signal encompassed multiple pipe-sensing strands on the pipe or in the trench separated by intermediate fiber sections which were spliced together at pull boxes at either end of the pipeline. By inspection, the start/end points of each relevant sensing strand were indexed, and the dataset was partitioned by strand. FBE power was compared between the four combinations of cable type and installation location to assess acoustic signal quality and identify channels with signals of interest.

These signals of interest were then evaluated using channel-specific spectrograms and magnitude spectra. Spectrograms visualize signal power spectral density (PSD) across frequencies and time. The spectrogram is computed using the short-time Fourier transform (STFT) with a Hann window $N_{window} = 2048$, overlap of 50%, and FFT size $N_{FFT} = 1024$.

$$S(t, f) = STFT(\tilde{x}_{ch}(t)) \quad (7)$$

PSD is then computed on the STFT across frequency and time and reported as decibels (dB/Hz).

$$PSD(t, f) = 10 \log_{10}(|S(t, f)|^2) \quad (8)$$

The magnitude spectrum visualizes signal magnitude M at various frequencies. The magnitude spectrum in decibels (dB) is computed on the FFT across the total signal frequency range.

$$M = 20 \log_{10}|X_{ch}(f)| \quad (9)$$

To compare different characteristic signals of interest, signal-to-noise (SNR) ratio was computed using root-mean-square amplitude of the signal A_{signal} and "noise" (absence of signal of interest) A_{noise} strain timeseries using the expressed as decibels (dB).

$$SNR = 20 \log_{10}\left(\frac{A_{signal}}{A_{noise}}\right) \quad (10)$$

3 DAS RESULTS

DAS measurements were performed continuously during a 1-hour pipeline commissioning procedure to capture acoustic signals during three characteristic processes (Figure 7):

1) water flow as the pipe is filled with water
2) pressure transient-related resonance vibrations
3) simulated leakage

First, time-domain signals during both characteristic processes were explored by visualizing FBE power across time and space. Waterfall plots of FBE power were created using DAS measurements from all signal channels along the 120-meter pipeline. Furthermore, to facilitate comparing DAS sensitivity between the four cable deployment configurations, signals from each were plotted in four stacked subplots.

Second, frequency-domain signals were investigated at the simulated leakage location at the uphill end valve. DAS measurements from channel 120 (location 120 meters) were selected for this purpose. Acoustic signal frequency content over time was explored with spectrograms. Signal baselines were assessed with time-independent magnitude spectra and quantified with signal-to-noise (SNR) ratio to compare between the four sensing cable configurations. Note, SNR was computed using the same strain amplitude signals used to compute the magnitude spectrum of the "signal" and "noise" spectrum. In full transparency, SNR was computed for the full pipe signal relative to the empty pipe noise (water flow detection), resonance signal relative to the no resonance noise (pressure transient detection), leaking pipe signal relative to the full pipe noise (leakage detection).

Ultimately, the objective of this proof-of-concept experimental setup was to explore DAS signals from fiber optic cables along a water distribution pipe in the context of local installation methods and environmental conditions.

Figure 7. DAS for water pipeline monitoring

DOI: 10.3217/978-3-99161-057-1-020

3.1 Water flow detection

DAS sensitivity to water flow inside the pipe during water filling was investigated. Water flowed into the empty pipe from the downhill end valve. The uphill end valve was open to air pressure. This resulted in a rising water level inside the inclined pipe (Figure 8). As the water level advanced up pipe, water flow and sloshing emitted vibrations and sound. This characteristic acoustic signal was detected and tracked across time along the pipeline. The spatiotemporal trend of 10 to 100 Hz frequency band extracted (FBE) reveals the advancing water level from the downhill end (location 0 m) to the uphill end (location approx. 120 m) (Figure 9). Signal visibility is best on tight-buffered cable on pipe, and progressively worse for other sensing configurations.

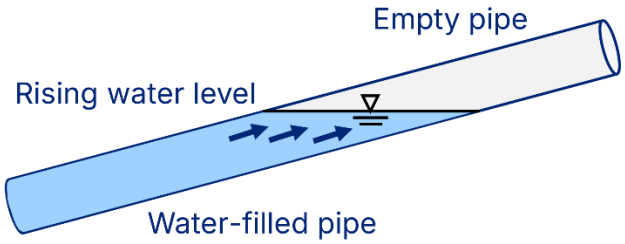

Figure 8. Pipe water flow condition

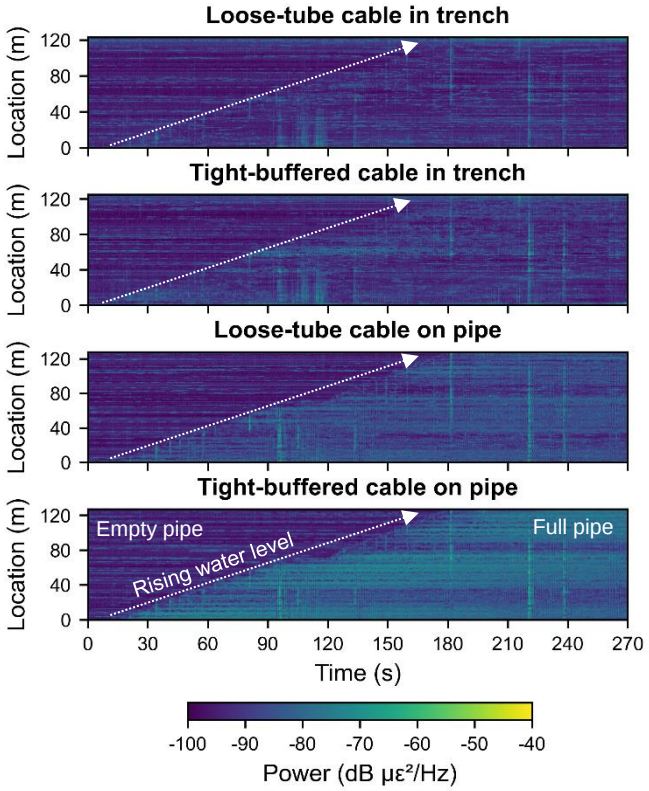

Figure 9. 10 to 100 Hz FBE power during pipe water filling

Spectrograms of frequency-domain signals at the uphill pipe end (location 120 m) reveal a characteristic jump in PSD at 0 to 400 Hz frequencies as the water level passes (Figure 10). This PSD signal is similarly visible on all sensing configurations. Differences in magnitude spectra before and after water level arrival highlight the relatively high SNR between the empty pipe noise floor and the water-filled pipe signal on all sensing configurations (Figure 11).

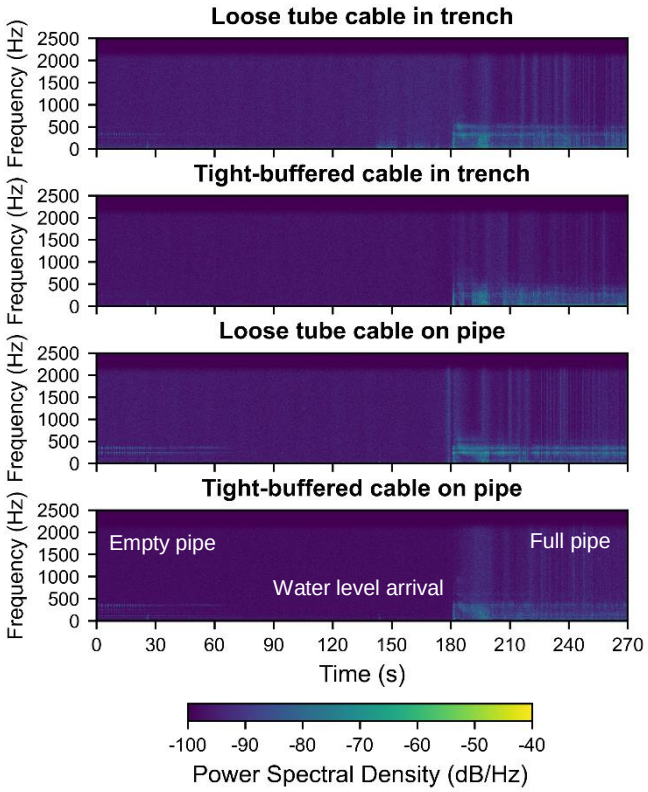

Figure 10. Spectrogram during passing water level

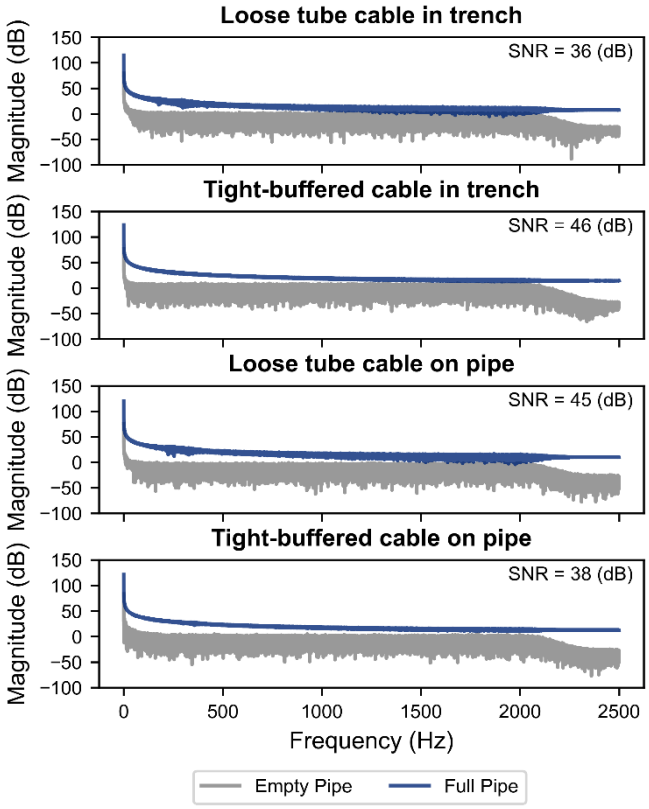

Figure 11. Magnitude spectra during passing water level

In short, DAS detected pipe water flow on all four sensing cable configurations. FBE Power signal is most visible on tight-buffered cable on pipe. Nonetheless, frequency-domain signal was relatively similar on all four sensing cable configurations.

DOI: 10.3217/978-3-99161-057-1-020

3.2 Pressure transient detection

DAS sensitivity to pipe water pressure transients was assessed. After the pipe was filled and the simulated leakage experiment was finished, the final steps of the pipeline commissioning procedure were performed. During this time, a water pressure transient was detected (Figure 12). FBE power from 2 to 20 Hz reveals a 10 second period of elevated acoustic signal along the entire pipeline (Figure 13). The resonant acoustic signal grows, stabilizes, and then disappears. It is most visible on the tight-buffered cable on the pipe, with progressively lower visibility on the other cable configurations.

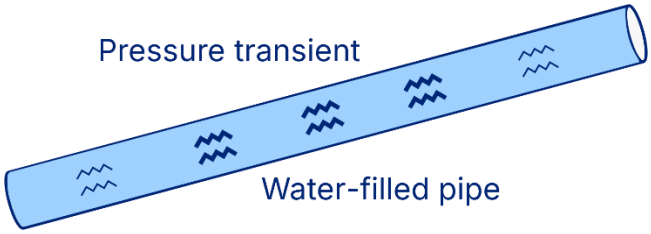

Figure 12. Pipe water pressure transient condition

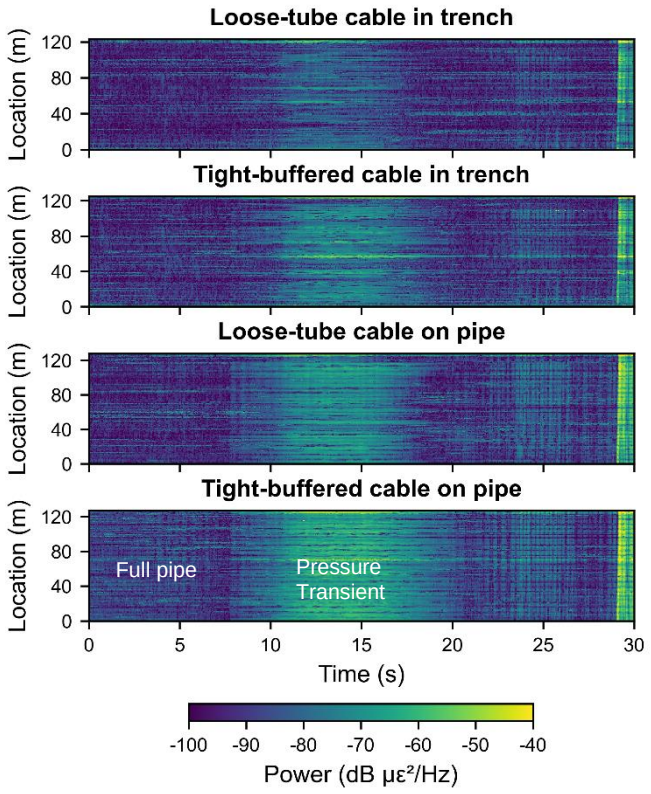

Figure 13. 2 to 20 Hz FBE power during pressure transient

Spectrograms at the uphill pipe end (location 120 m) reveal elevated PSD at low 0 to 20 Hz frequencies (Figure 14). PSD levels at higher frequencies remain relatively low and do not display a matching trend between the different sensing cables configurations. However, magnitude spectra reveal a much clearer difference between signals during the resonant pressure transient and the signal before without acoustic resonance (Figure 15). Both tight-buffered cables and the loose-tube cable on the pipe exhibited less noisy magnitude spectra and a higher SNR than the loose-tube cable in the trench.

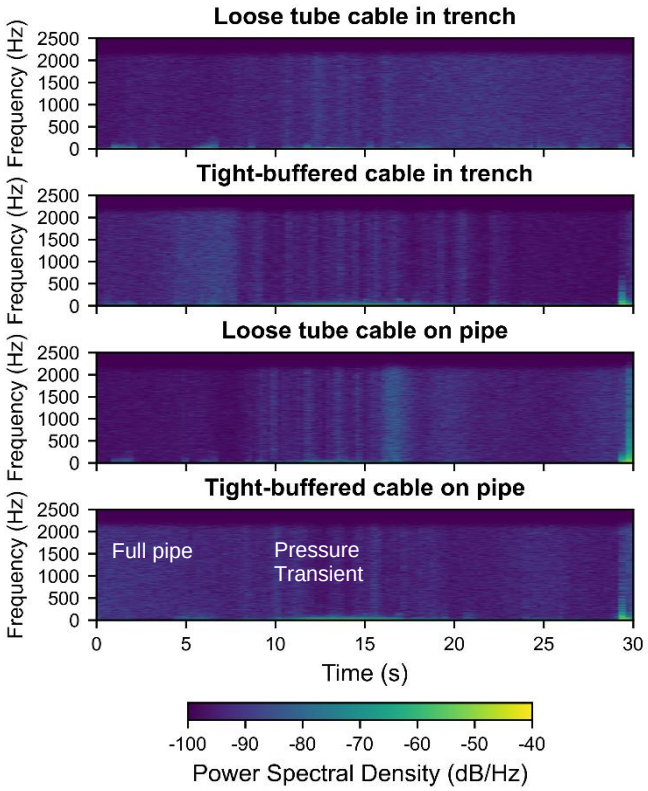

Figure 14. Spectrogram during pressure transient

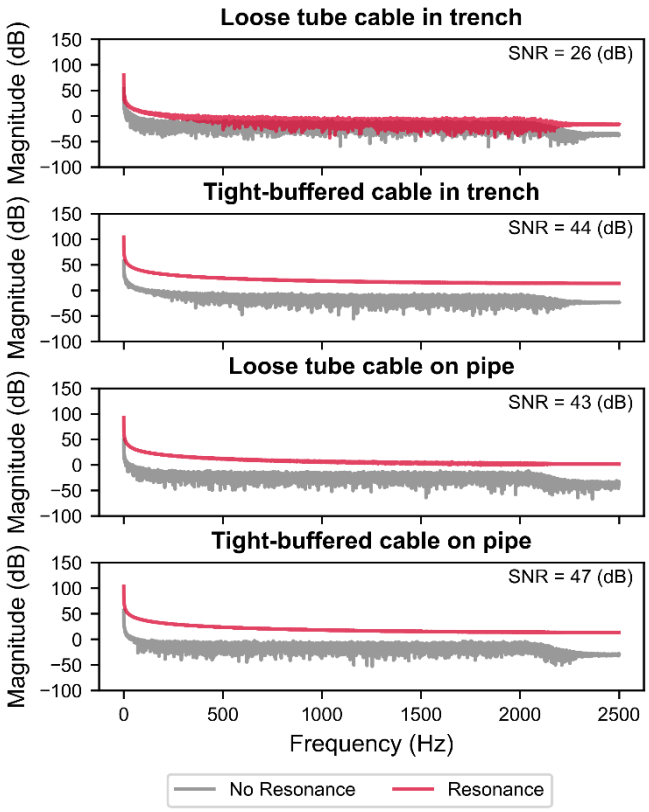

Figure 15. Magnitude spectra during pressure transient

In short, DAS detected a pipe water pressure transient on all four sensing configurations, albeit with lower SNR on loose-tube cable in the trench.

DOI: 10.3217/978-3-99161-057-1-020

3.3 *Leakage detection*

DAS sensitivity to pipe water leakage noise was evaluated. After the pipe was filled with water, water inflow increased by further opening the downhill end valve. This ensured water would escape from the open valve at the uphill pipe end to simulate high-flow leakage (Figure 16). Simulated leakage was maintained for 6 to 7 minutes until the downhill valve was closed. Water rushing through and exiting the pipe generated vibrations and sound. FBE power from 10 to 100 Hz highlights the start and end of the heavy water flow along the entire pipeline (Figure 17). FBE power was similarly visible on all four sensing configurations. As expected, the maximum acoustic signal was measured at the simulated leakage location.

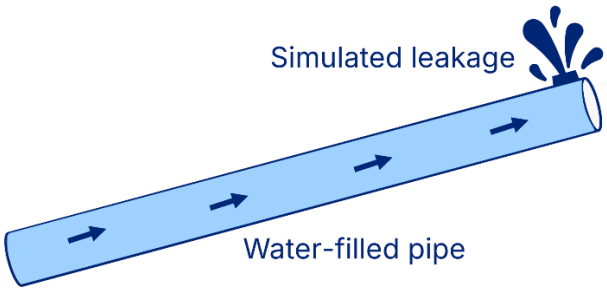

Figure 16. Pipe water leakage condition

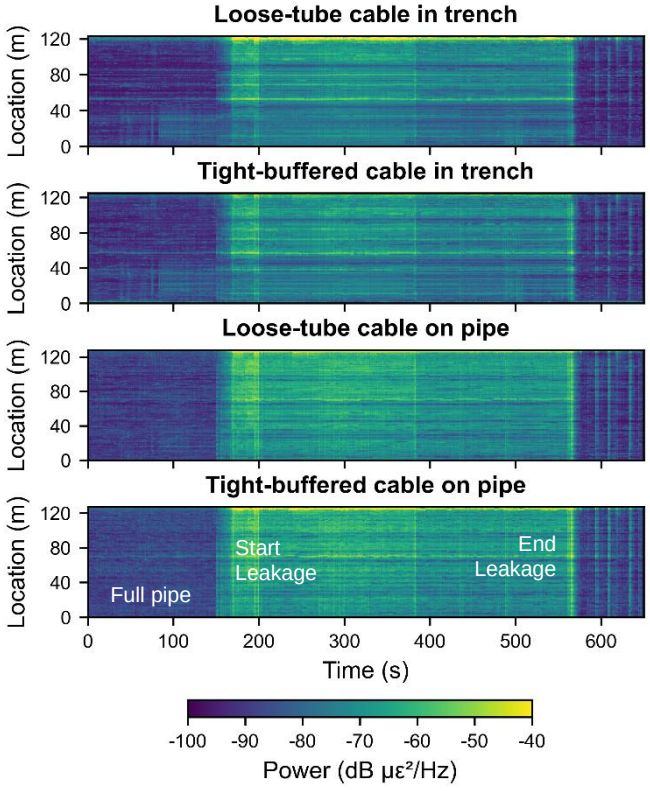

Figure 17. 10 to 100 Hz FBE power during simulated leakage

Spectrograms of frequency-domain signals at the simulated leakage location (location 120 m) display a striking jump in PSD at 0 to 400 Hz, and elevated PSD at 400 to 1000 Hz during simulated leakage (Figure 18) on all sensing cable configurations. Differences in magnitude spectra for signals from the full pipe and leaking pipe suggest a reasonably high SNR between the leaking pipe signal against the full pipe baseline (Figure 19).

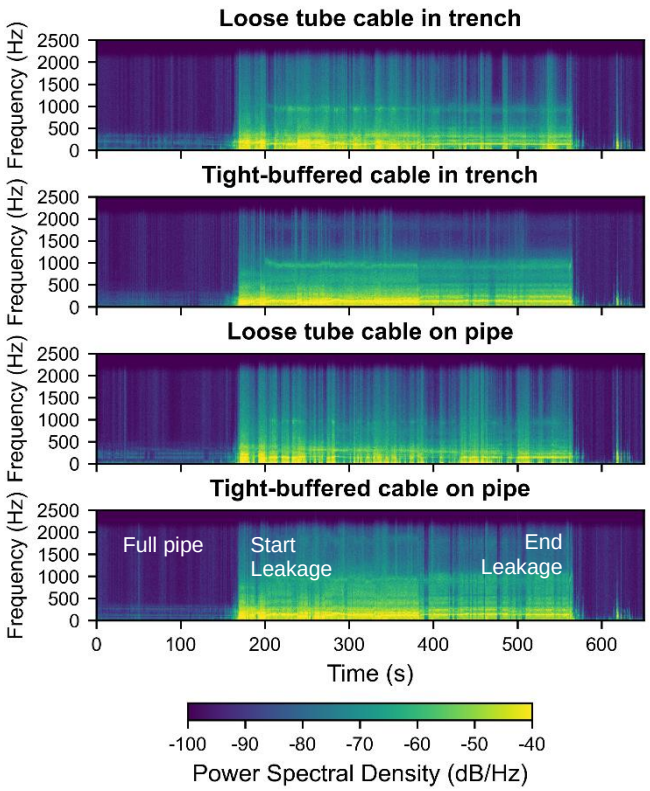

Figure 18. Spectrogram of channel at simulated leak

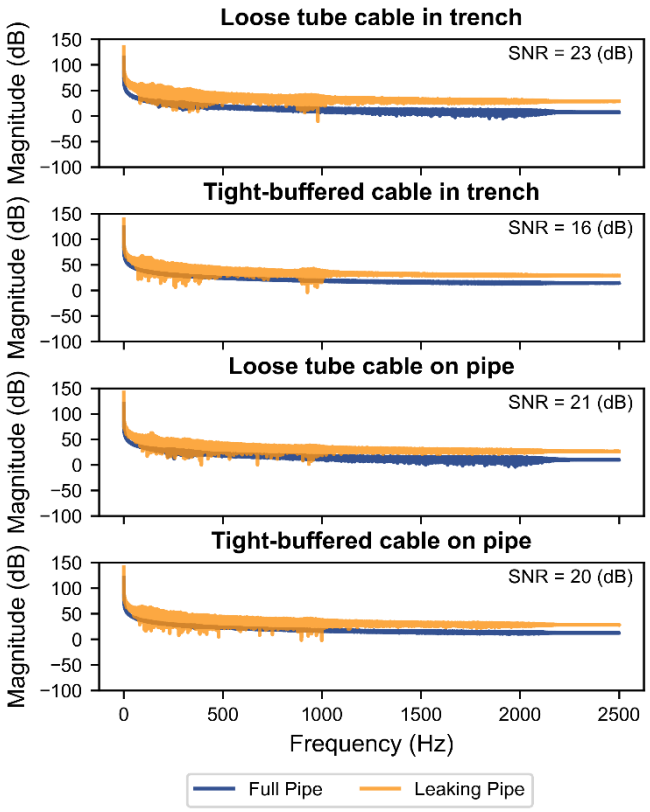

Figure 19. Magnitude spectra of channel at simulated leak

In short, DAS detected pipe water leakage on all four sensing configurations, with similar sensitivity on all four sensing cable configurations.

DOI: 10.3217/978-3-99161-057-1-020

To summarize, each of the three pipe signal states: 1) pipe water flow, 2) pressure transient-induced resonance, and 3) simulated leakage exhibited unique DAS data characteristics in terms of FBE power, spectrogram power spectral density, and magnitude spectrum trends.

Pipe-mounted cables exhibited a higher degree of FBE power sensitivity than trench-lain cables. Tight-buffered cables generally exhibited a higher degree of FBE power sensitivity than loose-tube cables. At the channel near the simulated leakage location, all sensing configurations exhibited relatively high frequency-domain signal visibility. Notably, trench-lain fibers turned out more sensitive than expected. Their high signal sensitivity was possible because they were located very close to the pipeline. This suggests that trench-lain fiber optic cables can offer sufficient DAS sensitivity to detect pipeline signals if the cables are located close to the pipeline.

4 DISCUSSION

Deploying DAS for water pipeline leakage monitoring presents a trade-off between DAS signal sensitivity and fiber optic cable deployment feasibility and cost (Figure 20).

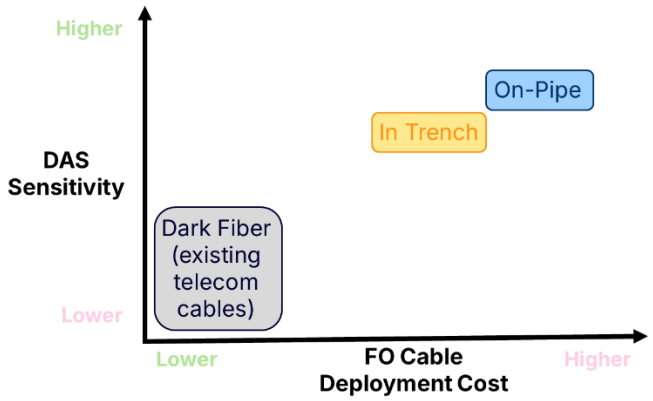

Figure 20. Qualitative comparison of DAS sensitivity to pipeline signals vs. fiber optic cable deployment cost

Mounting fiber optic sensing cables directly to the pipe offers superior DAS sensitivity. This is because pipeline acoustic signals can transmit directly to the fiber. However, this approach requires significant manual labor and installation logistics coordination. In short, it is a high-cost high reward approach appropriate for high resource deployment conditions such as new installations or retrofits for lifeline pipelines.

On the other hand, laying fiber optic sensing cables in the trench along the pipeline offers relatively lower DAS sensitivity. This is because pipeline acoustic signals need to travel through the trench backfill soil to reach the fiber. However, this approach requires less manual labor and is faster than attaching cables to the pipe. With reasonable DAS sensitivity, this medium cost approach may be a more feasible alternative for low resource deployment conditions. Nonetheless, both methods require resources and coordination to deploy sensing cables during pipeline construction excavations. They are therefore only usable if a DAS deployment is planned before pipeline construction activities.

Long term monitoring and maintenance are also a challenge. Although sensing cables typically have a long lifespan, when deployed in a pipeline alignment, they may be accidentally damaged during pipeline maintenance operations. Installing DAS interrogators in the field may be cost prohibitive given the need for power supply, climate control, and theft-prevention. From a scaling perspective, deploying sensing cables inside the pipeline alignment as done in this study can be difficult. Accordingly, it works best for critical pipelines with committed stakeholders in a supportive regulatory environment.

Alternatively, dark fiber DAS using existing buried telecommunications fiber optic cables is incredibly convenient with zero physical deployment installation and negligible maintenance costs. In this approach, a DAS interrogator is safely connected to an existing telecommunications cable network that runs from a datacenter through the pipeline network of interest. From a scaling perspective, a standardized dark fiber DAS method for detecting water pipeline leakage would offer a truly low cost and large-scale solution. However, this approach typically has lower DAS sensitivity given that existing cables may be far away from the monitored pipeline and may have poor acoustic signal coupling with subsurface soil. Therefore, further research is needed to better understand and improve dark fiber DAS sensitivity to pipe water leakage.

5 CONCLUSIONS

This study presents a reproducible workflow for DAS system deployment and signal processing for water pipeline leak detection in field conditions. The experimental configuration involved fiber optic sensing cables deployed directly in the pipeline alignment during construction. Both tight-buffered and loose-tube cables were installed on the pipe and in the trench. All four sensing cable configurations exhibited relatively high DAS sensitivity (high SNR) to pipeline acoustic signals during pipe water filling and simulated leakage. These results approximate a potential upper-bound for DAS sensitivity to water pipeline leak detection for each of the sensing cable configurations.

In contrast to other past work which simulated pipeline leakage in fully controlled laboratory conditions, this study consciously pursued the complete opposite approach to embrace the potentially high levels of uncertainty associated with deploying fiber optic cables and DAS in the field. In this context, we acknowledge this study is limited to a single location with a single pipeline and a single simulated leakage signal source. The presented optimistic results of high SNR for all sensing cable configurations near the simulated leakage may be due to supportive experimental conditions. Intuitively, all four deployed sensing cables were on or very close to the pipe, so they detected pipeline acoustic signals reasonably well. Had the sensing cables been further away, their DAS sensitivity to pipeline signals would likely have been reduced.

Further work will investigate DAS sensitivity for water pipeline leakage detection with sensing cable configurations where fiber-optic cables are further away from the pipeline of interest. This will help demonstrate the workflow is applicable to dark fiber conditions where DAS is deployed on existing buried telecommunications cables which may be not close to the monitored pipeline. Furthermore, additional testing in locations with different subsurface conditions (soil type, temperature, moisture), with various pipe materials and leakage mechanisms is needed to develop a comprehensive dataset of pipe water leakage noise signals. This will support a robust and

DOI: 10.3217/978-3-99161-057-1-020

adaptable workflow for dark fiber DAS to operationalize water pipeline leakage detection. This standardization effort can be scaled up with engagement from public agency stakeholders and regulators to ultimately transform the state of practice for water pipeline monitoring.

To summarize the main contributions of this work:

1. Developed reproducible framework for DAS system deployment and signal processing for water distribution pipeline monitoring.
2. Characterized influence of fiber optic cable type (tight-buffered vs. loose-tube) and installation location (on pipe vs. along pipe in trench) on DAS sensitivity to pipeline acoustic signals.
3. Explored time-domain and frequency-domain content of acoustic signals relevant to pipeline anomaly and leakage detection.

ACKNOWLEDGMENTS

The authors gratefully acknowledge the support of Dr. Yaobin Yang, Dr. Chien-Chih Wang, and James Xu (University of California, Berkeley), the East Bay Municipal Utility District (EBMUD), and the Berkeley Center for Smart Infrastructure (CSI).

REFERENCES

[1] Soga, K., & Luo, L. (2018). Distributed fiber optics sensors for civil engineering infrastructure sensing. Journal of Structural Integrity and Maintenance, 3(1), 1–21. https://doi.org/10.1080/24705314.2018.1426138

[2] Hubbard, P. G., Xu, J., Zhang, S., DeJong, M., Luo, L., Soga, K., Papa, C., Zulberti, C., Malara, D., Fugazzotto, F., Garcia Lopez, F., & Minto, C. (2021). Dynamic structural health monitoring of a model wind turbine tower using distributed acoustic sensing (DAS). Journal of Civil Structural Health Monitoring, 11(3), 833–849. https://doi.org/10.1007/s13349-021-00483-y

[3] Xu, J. T., Luo, L., Saw, J., Wang, C.-C., Sinha, S. K., Wolfe, R., Soga, K., Wu, Y., & DeJong, M. (2024). Structural health monitoring of offshore wind turbines using distributed acoustic sensing (DAS). Journal of Civil Structural Health Monitoring. https://doi.org/10.1007/s13349-024-00883-w

[4] Hubbard, P. G., Ou, R., Xu, T., Luo, L., Nonaka, H., Karrenbach, M., & Soga, K. (2022). Road deformation monitoring and event detection using asphalt-embedded distributed acoustic sensing (DAS). Structural Control and Health Monitoring, 29(11). https://doi.org/10.1002/stc.3067

[5] Saw, J., Zhu, X., Luo, L., Correa, J., Soga, K., & Ajo-Franklin, J. (2025). Distributed Fiber Optic Sensing for in-well hydraulic fracture monitoring. Geoenergy Science and Engineering, 250, 213792. https://doi.org/10.1016/j.geoen.2025.213792

[6] Gemeinhardt, H., & Sharma, J. (2024). Machine-Learning-Assisted Leak Detection Using Distributed Temperature and Acoustic Sensors. IEEE Sensors Journal, 24(2), 1520–1531. IEEE Sensors Journal. https://doi.org/10.1109/JSEN.2023.3337284

[7] Muggleton, J. M., Hunt, R., Rustighi, E., Lees, G., & Pearce, A. (2020). Gas pipeline leak noise measurements using optical fibre distributed acoustic sensing. Journal of Natural Gas Science and Engineering, 78, 103293. https://doi.org/10.1016/j.jngse.2020.103293

[8] Saw, J., Luo, L., Chu, K., Ryan, J., Soga, K., & Wu, Y. (2025). Distributed Acoustic Sensing for Whale Vocalization Monitoring: A Vertical Deployment Field Test. Seismological Research Letters. https://doi.org/10.1785/0220240389

[9] Araica, K. (Moita), Cicala, G., McLeod, M. P., Soga, K., Jasiak, M., Hubbard, P., Wang, C.-C., Yang, Y., Luo, L., Yeskoo, A., & Chiu, S.-H. (2024). Design and Installation of Distributed Fiber Optic Sensing Technology to Monitor HDPE Pipelines at an Earthquake Fault Crossing. Pipelines 2024, 561–571. https://doi.org/10.1061/9780784485569.060

[10] Chiu, S.-H., Jasiak, M., Dong, C., Banushi, G., Soga, K., Riemer, M., Katzev, D., Wham, B., Berger, B., Mason, J., & O'Rourke, T. (2025). Design of Distributed Fiber Optic Sensing Monitoring System for Earthquake-Resistant Ductile Iron Pipelines Crossing Seismic Fault. 567–575. https://doi.org/10.1061/9780784485996.055

[11] Chiu, S.-H., Zhang, Q., Soga, K., Takhirov, S., Cha, W., Katzev, D., & Mason, J. (2024). Performance Evaluation of Earthquake Resistant Ductile Iron Pipe Joints Using Combined Experimental and Numerical Method. 261–271. https://doi.org/10.1061/9780784485583.028

[12] Yu, B., & Barter, R. L. (2024). Veridical data science: The practice of responsible data analysis and decision making. MIT Press. https://vdsbook.com/

[13] Lu, B., Pan, Z., Wang, Z., Zheng, H., Ye, Q., Qu, R., & Cai, H. (2017). High spatial resolution phase-sensitive optical time domain reflectometer with a frequency-swept pulse. Optics Letters, 42(3), 391-394. https://doi.org/10.1364/OL.42.000391

[14] Eickhoff, W., & Ulrich, R. (1981). Optical frequency domain reflectometry in single-mode fiber. https://doi.org/10.1063/1.92872
Oppenheim, A. V., Buck, J. R., & Schafer, R. W. (1999). Discrete-time signal processing (2nd ed.). Prentice Hall. https://books.google.com/books?id=cR3CQgAACAAJ

[15] Saw, J. (2025). Listening with Light: Distributed Acoustic Sensing for Event Detection, Characterization, and Classification (Doctoral dissertation). University of California, Berkeley.